

The role of spin-orbit coupling in topologically protected interface states in Dirac materials

D. S. L. Abergel¹

Jonathan M. Edge¹

Alexander V. Balatsky^{1,2}

¹ Nordita, KTH Royal Institute of Technology and Stockholm University, Roslagstullsbacken 23, SE-10691 Stockholm, Sweden

² Los Alamos National Laboratory, Los Alamos, NM 87545, USA

PACS numbers: 73.20.-r, 73.40.-c

Abstract. We highlight the fact that two-dimensional materials with Dirac-like low energy band structures and spin-orbit coupling will produce linearly dispersing topologically protected Jackiw-Rebbi modes at interfaces where the Dirac mass changes sign. These modes may support persistent spin or valley currents parallel to the interface, and the exact arrangement of such topologically protected currents depends crucially on the details of the spin-orbit coupling in the material. As examples, we discuss buckled two-dimensional hexagonal lattices such as silicene or germanene, and transition metal dichalcogenides such as MoS₂.

Keywords: Dirac materials, interface states, persistent currents, topological protection.

1. Introduction

A major issue in contemporary condensed matter physics is the attempt to produce and control currents which are polarized in one or more of several spin-like degrees of freedom, and which can be used for switching and possibly quantum computing applications. The real electron spin was initially proposed for this, leading to the moniker “spintronics” [1] and many advances in commercially relevant technologies. Recently, the isolation of two-dimensional (2D) hexagonal crystals with their two inequivalent valleys and two inequivalent lattice sites have lead to the suggestion of using these degrees of freedom in an analogous way in so called “valleytronics” [2] and “pseudospintronics” [3] applications. In general, one way to create polarization in one of these spin-like degrees of freedom is to break a symmetry of a system such that the degeneracy of the two spin-like flavors is lifted and transport is only permitted for one flavor, for example using the giant magneto-resistance effect [4]. Another way is to utilize differences in how each flavor behaves under an external perturbation [5]. A third way is to employ the topological properties of materials in order to engineer spatially localized states which can be manipulated via the topology of the underlying material. One such example of this is the 2D surface state which forms at the interface between bulk Bi_2Se_3 crystals and the vacuum [6, 7], where the change in the Z_2 invariant from the crystal to the vacuum implies that there must be a local closing of the band gap and an associated interface mode. These interface modes are protected against disorder because the change in the topological nature of the material on either side of the interface requires the presence of such metallic surface states.

In this article, we investigate the details of a localized and controllable version of the phenomenon of current polarization enforced by topological change in Dirac materials [8]. Localized interface modes protected by topological changes induced by a change in sign of the band mass at the boundary of a system are known as “Jackiw-Rebbi modes” [9]. ‡ These interface modes support persistent currents which can, in principle, be utilized for electronic control and switching applications, and may lead to significant efficiency improvements over conventional charge switching technology [10]. Bilayer graphene was considered in a similar context [11, 12], and complementary results were shown, including proposals to manipulate such states in “electronic highways” [13]. Also, such modes can be hosted by the staggered sublattice potential associated with the interface between graphene and hexagonal boron nitride [14], and in certain perovskite materials [15].

Our analysis corresponds to a different class of system where the underlying band structure is governed by the linear Dirac Hamiltonian, and we wish to highlight a fundamentally different feature, namely that the details of the spin-orbit coupling (SOC) play a crucial role in determining specific properties of the interface modes. In particular, the variety of behavior seen in different materials caused by the interplay between the

‡ Other authors have labeled these modes as “topologically confined modes” and “topological zero line mode”.

SOC and other effects related to the lattice gives a handle for selecting the properties of interface modes for specific applications.

For clarity, in the remainder of this introduction we demonstrate that in the generic case where there is a band gap at the Fermi energy and a finite quasiparticle mass, arranging a system such that there is an interface where the Dirac mass is positive on one side and negative on the other will ensure that topologically protected modes are present at the interface. Then, in Sec. 2 we shall show that the persistent spin or valley currents carried by these interface modes depend on the detailed nature of the SOC and the interplay between the SOC and the sublattice asymmetry in each specific material. Section 3 contains our conclusions and some discussion.

To illustrate the general point of topological modes confined by mass inversion, the Hamiltonian for the bulk of a generic hexagonal lattice can be written for a single valley and spin as

$$H = \hbar v(\hat{k}_x \tau_x + \hat{k}_y \tau_y) + \Delta \tau_z, \quad (1)$$

where Δ is the Dirac mass, $\hat{k}_x = -i\partial_x$ and $\hat{k}_y = -i\partial_y$ are the wave vector operators, v is the Fermi velocity, and $\tau_{x,y,z}$ are Pauli matrices in the sublattice space. We begin by demonstrating that changing the sign of the band mass $\Delta \rightarrow -\Delta$ in the bulk will alter the topological properties of this toy system. The topological quantum number associated with a Hamiltonian such as Eq. (1) is the Chern number $C(\Delta)$ [16]. It may be expressed as an integral of the Berry curvature over the Brillouin zone and for a system described by $H = \sum_i d_i(\mathbf{k})\tau_i$ [the Hamiltonian in Eq. (1) has $\mathbf{d} = (\hbar v \hat{k}_x, \hbar v \hat{k}_y, \Delta)$], the Chern number can be calculated from [17, 18]

$$\begin{aligned} C(\Delta) &= \frac{1}{4\pi} \left(\int_0^\Lambda d^2\mathbf{k} + \int_{|\mathbf{k}|>\Lambda} d^2\mathbf{k} \right) \epsilon^{\mu\nu\lambda} \bar{d}_\mu \partial_{k_x} \bar{d}_\nu \partial_{k_y} \bar{d}_\lambda \\ &= C^{(1)}(\Delta, \Lambda) + C^{(2)}(\Delta, \Lambda). \end{aligned} \quad (2)$$

In this equation, we have split the integration into two contributions. The first, $C^{(1)}$, comes from wave vectors near to the gapless point, and the second, $C^{(2)}$, from the rest of the Brillouin zone where we assume there are no further gap closings. A cut-off Λ distinguishes these two regions, $\bar{\mathbf{d}} = \mathbf{d}/|\mathbf{d}|$, and ϵ is the three-dimensional Levi-Civita symbol. We examine the change in the Chern number δC when the Dirac mass is inverted by calculating $\delta C = C(\Delta) - C(-\Delta)$ so that a finite value of δC indicates a change in the system's topological properties. We know that the region of k -space near the gapless point is the only place where the conduction and valence bands come near to each other, and that the gapped part of a Hamiltonian cannot introduce a change in the Chern number. Hence, δC may be computed solely from the low-momentum part of Eq. (2). Hence, $\delta C = C^{(1)}(\Delta) - C^{(1)}(-\Delta)$ and, in the limit $\Delta \rightarrow 0$ and $\Lambda \gg \Delta/(\hbar v)$, we obtain

$$\delta C = \frac{1}{4\pi} \int_0^\Lambda \frac{2\hbar^2 v^2 \Delta}{(\hbar^2 v^2 |\mathbf{k}|^2 + \Delta^2)^{3/2}} d^2 k = 1. \quad (3)$$

Therefore, since there is a change in the Chern number when the sign of Δ is reversed,

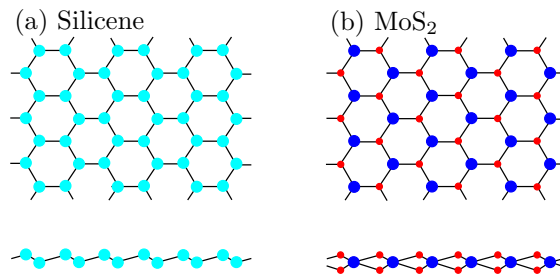


Figure 1. Lattice structures of (a) silicene, and (b) molybdenum disulphide, showing both a top-down view (upper sketch) and side-on view (lower sketch).

the boundary between regions of a system with $\Delta > 0$ and $\Delta < 0$ hosts a topologically protected interface state. §

We now demonstrate the localization of a linear “interface mode” in the region where the band mass changes sign. This corresponds exactly to the Jackiw-Rebbi modes introduced earlier [9]. We allow the mass term to become inhomogeneous, such that it is constant in the y direction, but has linear slope in the x direction with $\Delta(0) = 0$ then $\Delta(\mathbf{r}) = \Delta_0 x/R$ so that $1/R$ characterises the gradient of the change in the mass and a one-dimensional domain wall is defined. The spectrum of this system is found by rotating the Hamiltonian with the unitary operator $U = e^{i\pi\tau_x/4}$. Since \hat{k}_y commutes with the Hamiltonian, we replace it with the eigenvalue k_y and hence $H' = -i\hbar v\partial_x\tau_x + \hbar v k_y\tau_z - \Delta_0 x\tau_y/R$. The off-diagonal elements can now be written in the form of ladder operators $a = \sqrt{\alpha/2}(x + \partial_x/\alpha)$ and $a^\dagger = \sqrt{\alpha/2}(x - \partial_x/\alpha)$ with $\alpha = \Delta_0/(\hbar v R)$ which act on the harmonic oscillator functions Φ_n as $a^\dagger\Phi_n = \sqrt{n+1}\Phi_{n+1}$, $a\Phi_n = \sqrt{n}\Phi_{n-1}$, and $a\Phi_0 = 0$. We can construct by inspection an eigenvector of H' which has the form

$$\Psi = e^{ik_y y} \begin{pmatrix} \Phi_0 \\ 0 \end{pmatrix}$$

and dispersion $\varepsilon = \hbar v k_y$. This mode behaves as zero gap semiconductor despite the mass gap in the bulk system, and is topologically protected by the change in the Chern number across the domain wall.

2. Real systems

The precise details of the manifestation of the topologically protected interface states will depend on the microscopic characteristics of the material in which they are realized, so we give two examples of physical systems which fulfil the requirements outlined above.

§ Note that there is some subtlety associated with this analysis, as described in Ref. [12]. But the change in Chern number across a domain wall is a well-defined topological invariant in the cases we consider.

2.1. Silicene

The first, silicene, has already been discussed in the context of interface modes [19, 20], although valley currents were not mentioned. Theoretical proposals for transport through normal-ferromagnetic-normal junctions [21] and gated regions [22] which produce spin or valley currents have been reported, but this is a fundamentally different mechanism from the interface state transport we discuss. For silicene, the τ_z term in the Hamiltonian represents the combination of the SOC and the asymmetry between the on-site potential of the two sublattices in the hexagonal crystal. The SOC term enters with the τ_z Pauli matrix because the warping of the lattice which generates the coupling is opposite on the two sublattices [23]. Also, because silicene exhibits a buckled structure [as illustrated in Fig. 1(a)], applying a transverse electric field adjusts the static potential on the two sublattices in different magnitude, hence modifying the mass. Silicene is known to have a rich phase diagram in the non-interacting regime [20] in which varying the transverse electric field causes the 2D bulk to undergo a phase transition from a quantum anomalous Hall phase to a band insulator phase due to the change in the Dirac mass. In common with all materials that have a 2D hexagonal lattice, silicene exhibits the valley pseudospin in addition to the real electron spin and lattice pseudospin. The low-energy effective Hamiltonian for electrons of spin $s = \pm 1$ in valley $\xi = \pm 1$ of silicene is [23]

$$H_{\xi s}^{\text{Sil}} = \hbar v (\hat{k}_x \tau_x - \xi \hat{k}_y \tau_y) + \xi s \lambda \tau_z + \frac{l E_z}{2} \tau_z \quad (4)$$

where v is the Fermi velocity associated with the Dirac spectrum, the Pauli matrices $\tau_{x,y,z}$ are in the sublattice space, λ parameterizes the strength of the SOC, $l E_z$ is the contribution to the band gap induced by external gating, and $\hat{k}_i = -i \hbar \partial_{x_i}$ is the operator for the electron wave vector. The inhomogeneous electric field is assumed to define an interface oriented along the y axis at $x = 0$, and is represented as $E_z = x \mathcal{E} / R$. The effective mass of the Dirac fermions is negative when $l E_z(x) < -\xi s \lambda$, and positive otherwise. Therefore, for bands with $\xi s = 1$, there are interface modes confined near $x = -\lambda R / (\mathcal{E} l)$ and a further two modes with $\xi s = -1$ near $x = \lambda R / (\mathcal{E} l)$. This is a difference from our toy example discussed above, where the band was localized near $x = 0$, and is due to the combination of the intrinsic SOC in silicene and the electric field in creating the total Dirac mass. To find the dispersion of these interface modes, we apply the same series of manipulations as in our toy system which yields $\varepsilon_{\xi s}^{\text{Sil}} = -\xi \hbar v k_y$.

We can use a topological characteristic to describe the spectral asymmetry of the Hamiltonian which is enforced by the topological modes. We define the indices [24]

$$\eta_s = \frac{2}{\sqrt{\pi}} \text{Tr} \int_0^\infty H e^{-y^2 H^2} P_s dy \quad (5)$$

$$\eta_\xi = \frac{2}{\sqrt{\pi}} \text{Tr} \int_0^\infty H e^{-y^2 H^2} P_\xi dy \quad (6)$$

where P_s and P_ξ are, respectively, the projection operators onto spin s and valley ξ . The notation Tr denotes a sum over all spins and valleys. This index counts the

excess number of bands with positive energy. As shown in Fig. 2(a), applying this definition to the topological bands of the Hamiltonian in Eq. (4) gives $\eta_K = 2\text{sgn}(k_y)$ and $\eta_{K'} = -2\text{sgn}(k_y)$ because the electrons in valley K and in valley K' have opposite sign of their energy for a given k_y . This index indicates that there is a fundamental asymmetry in the valley distribution of the interface modes in silicene. Conversely, the spin characteristic is zero because of the degeneracy of the bands.

We can also describe one-dimensional spin or valley currents along the interface in terms of the group velocity of electrons in each band. For a single band,

$$j_{\xi s} = \frac{1}{2\hbar k_c} \int_{-k_c}^{k_c} dk_y v_{\xi s} n_{\xi s}$$

where $v_{\xi s} = d\varepsilon_{\xi s}^{\text{Sil}}/dk_y$, $n_{\xi s}(k_y)$ is the occupation of the state with wave vector k_y in the band with indices ξ and s , and k_c is a cutoff wave vector of the order of the Brillouin zone size. Then, the total spin and total valley currents including the contributions from all topological bands are

$$\begin{aligned} j_s &= j_{K\uparrow} + j_{K'\uparrow} - j_{K\downarrow} - j_{K'\downarrow}, \\ j_\xi &= j_{K\uparrow} + j_{K\downarrow} - j_{K'\uparrow} - j_{K'\downarrow}. \end{aligned}$$

where we have adopted the convention that \uparrow -spin (K valley) electrons moving in the positive y direction give a positive contribution to the total spin (valley) current. In the case of silicene, the K valley electrons are all left-moving (with $v_{Ks} = -v$), while the K' electrons are all right moving (with $v_{K's} = v$), clearly indicating that there is a valley current $j_\xi = -2v$ at half filling. The sign of this current can be reversed by inverting the gradient of the electric field. The higher energy bands are quadratic and degenerate in spin and valley so do not contribute to the current. If a finite chemical potential μ is introduced so that the system is shifted away from half filling, a correction of $-2\mu/(\hbar k_c)$ is added to the current. Since $\hbar v k_c \gg \mu$ by definition, this effect is small indicating that the valley current is robust against realistic changes in the density.

Silicene has been experimentally isolated [25], but the disadvantage of this material is that the SOC is relatively small ($\lambda \approx 4\text{meV}$). The SOC in a buckled lattice made from germanium is an order of magnitude larger [23], and for the interface modes we are discussing, stronger SOC has the advantage of allowing a wider intrinsic gap between the bulk bands. Therefore, the interface modes we discuss would be easier to detect in that material.

2.2. Transition metal dichalcogenides

The second system we present is transition metal dichalcogenides (TMDs) such as MoS_2 . These materials are constructed of a hexagonal bipartite lattice where a sheet of transition metal atoms on the A sublattice are surrounded by two sheets of chalcogen atoms on the B sublattice, as shown in Fig. 1(b). The SOC comes primarily through the interaction with the heavier transition metal atom [26, 27], and so the coupling is asymmetric in the lattice sites, in contrast to the case of silicene. Hence we expect that

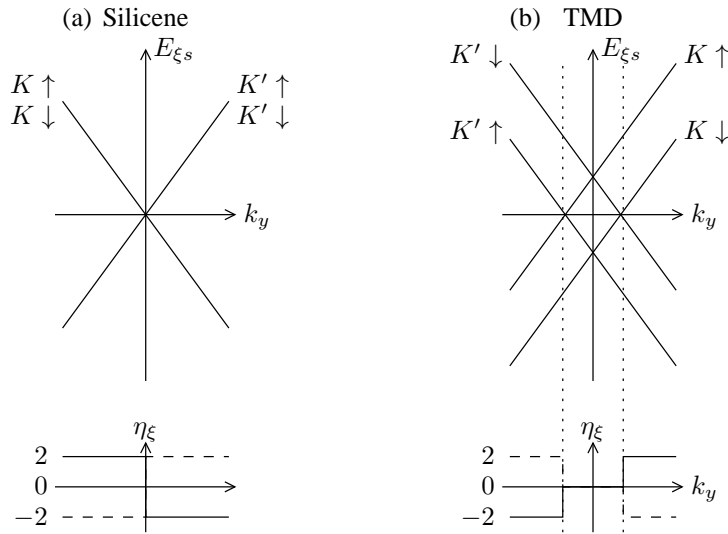


Figure 2. (a) The topologically protected interface modes in silicene. The two spin states in each valley are degenerate. (b) The topologically protected bands in TMDs. The lower plots in (a) and (b) show the valley band asymmetry parameter $\eta_{\xi}(k_y)$ for $\xi = K$ (solid lines) and $\xi = K'$ (dashed lines).

there may be differences in the manifestation of the topological modes. The low-energy effective Hamiltonian in the bulk is [28]

$$H_{\xi s}^{\text{TMD}} = \hbar v(\xi k_x \tau_x + k_y \tau_y) + \frac{\Delta}{2} \tau_z - \frac{\xi s \lambda}{2} (\tau_z - \tau_0). \quad (7)$$

where the band mass $\Delta \approx 1.6\text{eV}$ is a parameter of the lattice coming from the intrinsic chemical asymmetry between the two sublattices. The band mass is assumed to vary in space, with the same one-dimensional form $\Delta(x) = \Delta_0 x/R$ as was taken in the silicene case.|| The rotation of the Hamiltonian distributes the SOC term over τ_y and τ_0 so that the parameter λ enters the dispersion of the interface modes as $\varepsilon_{\xi s}^{\text{TMD}} = \xi \hbar v k_y + \xi s \lambda/2$. This indicates that the band spin asymmetry index is $\eta_s = 0$ for all k_y , but that the valley index η_{ξ} is finite for $|k_y| > \lambda/(2\hbar v)$ [see Fig. 2(b)]. This illustrates the fact that the arrangement of the interface modes is different from silicene because of the different nature of the SOC. A finite valley current exists with, $j_{\xi} = 2v + 2\mu/(\hbar k_c)$ which can also be reversed by switching the sign of the gradient of the inhomogeneous band mass. In contrast with silicene, we also have an overall spin current with $j_s = -\lambda/(\hbar k_c)$ which is set by the magnitude of the SOC. This current does not depend on the location of the chemical potential.

3. Conclusions

In conclusion, we have demonstrated that the design and control of mass inversion via careful selection of the host material for its band gap and SOC is a theoretically

|| However, we cannot suggest a physical mechanism for achieving this spatial variation.

viable technique for the creation and manipulation of topologically protected modes that may carry spin or valley polarized currents. In silicene, the interface modes carry valley current which can be controlled by local gating, and (if a mechanism for band inversion can be found) TMDs such as MoS₂ will exhibit both spin and valley currents at interfaces. The direction of these currents can be manipulated by reversing the sign of the gradient of the mass inhomogeneity. The topological protection we discuss is robust so long as there is no inter-valley scattering. This is because the derivation of Eq. (3) assumes that there is only one gapless point. However, for realistic systems with hexagonal lattice structure, there is a gapless point at each of the six Brillouin zone corners (*i.e.* one gapless point in each valley). We note that if the valleys are connected, the assumptions inherent in Eq. (3) are not satisfied. Thus, short-range scatterers such as lattice defects will be severely detrimental to the existence of interface modes.

Acknowledgments

This work was supported by ERC DM-321031 and by Nordita.

References

- [1] Žitúć I, Fabian J, and Das Sarma S, *Rev. Mod. Phys.* **76**, 323 (2004).
- [2] Rycerz A, Tworzydło J, and Beenakker CWJ, *Nat. Phys.* **3**, 172 (2007).
- [3] Pesin D, and MacDonald AH, *Nat. Mat.* **11**, 409 (2012).
- [4] Prinz GA, *Science* **282**, 1660 (1998).
- [5] Abergel DSL, and Chakraborty T, *Appl. Phys. Lett.* **95**, 062107 (2009).
- [6] Xia Y, Qian D, Hsieh D, Wray L, *et al.*, *Nat. Phys.* **5**, 398 (2009).
- [7] Zhang H, Liu C-X, Qi X-L, Dai X, *et al.*, *Nat. Phys.* **5**, 438 (2009).
- [8] Wehling T, Black-Schaffer A, and Balatsky AV, *Adv. Phys.* (Submitted) (2014).
- [9] Jackiw R and Rebbi C, *Phys. Rev. D* **13**, 3398 (1976).
- [10] Qiao Z, Jung J, Lin C, MacDonald AH, and Niu Q, arXiv:1302.6307 (Unpublished).
- [11] Martin I, Blanter Ya, and Morpurgo AF, *Phys. Rev. Lett.* **100**, 036804 (2008).
- [12] Li J, Morpurgo AF, Buttiker M, and Martin I, *Phys. Rev. B* **82**, 245404 (2010).
- [13] Qiao Z, Jung J, Niu Q, and MacDonald AH, *Nano Lett.* **11**, 3453 (2011).
- [14] Jung J, Qiao Z, Niu Q, and MacDonald AH, *Nano Lett.* **12**, 2936 (2012).
- [15] Liang Q-F, Wu L-H, and Hu X, *New J. Phys.* **15**, 063031 (2013).
- [16] Ryu S, Schnyder AP, Furusake A, and Ludwig AWW, *New J. Phys.* **12**, 065010 (2010).
- [17] Thouless D, Kohmoto M, Nightingale M, and den Nijs M, *Phys. Rev. Lett.* **49**, 405 (1982).
- [18] Qi X-L, Hughes TL, and Zhang SC, *Phys. Rev. B* **78**, 195424 (2008).
- [19] Ezawa M, *New J. Phys.* **14**, 033003 (2012).
- [20] Ezawa M, *Phys. Rev. B* **87**, 155415 (2013).
- [21] Yokoyama T, *Phys. Rev. B* **87**, 241409 (2013).
- [22] Tsai W-F, Huang C-Y, Chang T-R, Lin S *et al.*, *Nat. Commun.* **4**, 1500 (2013).
- [23] Liu C-C, Jiang H, and Yao Y, *Phys. Rev. B* **84**, 195430 (2011).
- [24] Balatsky AV, *JETP Lett.* **47**, 746 (1988).
- [25] Vogt P, De Padova P, Quaresima C, Avila J, *et al.*, *Phys. Rev. Lett* **108**, 155501 (2012).
- [26] Kormányos A, Zólyomi V, Drummond ND, Rakyta P, *et al.*, *Phys. Rev. B* **88**, 045416 (2013).
- [27] Rostami H, Moghaddam AG, and Asgari R, *Phys. Rev. B* **88**, 085440 (2013).
- [28] Xiao D, Liu G-B, Feng W, Xu X *et al.*, *Phys. Rev. Lett.* **108**, 196802 (2012).